Recent Advances in Electromagnetic Encoders for Motion Sensing and Chipless-RFID

Amirhossein Karami-Horestani, Ferran Paredes, and Ferran Martín
CIMITEC, Departament d'Enginyeria Electrònica, Universitat Autònoma de Barcelona, 08193 Bellaterra, Spain

Abstract

This paper reviews the recent advances in electromagnetic encoders for motion sensing and near-field chipless-RFID. The reported encoders exhibit more than one bit of information per encoder position (or row), and the main target in the research activity carried out by the authors has been to maximize such number of bits per encoder position, a Figure of Merit (FoM), as much as possible. It is shown that, for that purpose, it is necessary to encode not only in time (the former procedure), but also in frequency, in phase, or in frequency and phase simultaneously. Various prototype examples are reported in the paper. The highest achieved FoM is 8.78 bits per encoder position.

1. Introduction

Electromagnetic encoders constitute an alternative to optical encoders [1], magnetic encoders [2,3] and Hall-effect sensors [4-7] for the measurement of medium/high range displacements and velocities. Moreover, electromagnetic encoders can be applied to the implementation of near-field chipless-RFID systems with sequential bit reading. These encoders consist of at least a chain (linear or circular) of inclusions (typically metallic, although dielectric inclusions are also possible) printed or etched on a dielectric substrate (ceramic, plastic, organic, etc.), and a reader. For retrieving the information relative to the ID code (for chipless-RFID applications) or encoder motion (as a motion sensor), the encoder must be displaced over the sensitive part of the reader at short distance (airgap), so that the information provided by the inclusions can be obtained sequentially. This means that the reader must contain an element sensitive to the presence of inclusions. Such element is typically a transmission line-based structure, and the working principle is based on the variation of the amplitude or phase of the transmission or reflection coefficient of such structure at the operating frequency/ies.

The former reported electromagnetic encoders were implemented with a single chain of inclusions (linear or circular), and encoding was merely based on the presence (logic state '1') or absence (logic state '0') of functional inclusions [8,10]. These encoders were useful as near-field chipless-RFID tags, or time-domain signature barcodes (the designation used in [11]), where the ID was inferred sequentially in a time-division multiplexing scheme. Nevertheless, by considering that all the inclusions are present at their predefined positions (periodic), such encoders can be applied to the determination of encoder velocity (from the time lapse between adjacent pulses) and displacement (from the cumulative number of pulses from a reference position) [12]. As motion sensors, such encoders are incremental (not absolute) since, after a system reset, the encoder must return to the reference position. The limitation as near-field chipless-RFID tags (with an arbitrary number of functional inclusions at the predefined positions) concerns the fact that such encoders are not synchronous and hence for retrieving the ID code, the displacement velocity of the encoder must be known.

Soon after these former encoders, synchronous electromagnetic encoders were proposed [13]. These encoders were based on a chain of inclusions with a certain ID code, and a periodic chain (clock chain), which dictates the instants of time for retrieving the ID information. In such encoders, the number of bits per position is one, and for that reason they are not absolute encoders (as many states per position as different number of discrete positions are needed in an absolute encoder). However, it was demonstrated in [13] that by encoding the whole encoder with the so-called De Bruijn sequence, any subset of a certain number of bits, *N*, does not repeat, and therefore such encoders can provide the absolute position after they have moved such number of *N* positions. Such encoders have been designed as quasi-absolute encoders. For the implementation of true absolute encoders, it is thus necessary to increase the number of bits per encoder position, and this has been the main target of our research in the last years. Let us next discuss such approaches.

2. Strategies to Enhance the Number of Bits per Encoder Position

2.1 Time/Frequency Domain Encoders

The idea behind this approach is to consider inclusions of different size, corresponding to resonant elements of different frequency. In the simplest implementation, with a single chain, the number of states per position, and hence the number of bits, is dictated by the number of different inclusions' sizes, particularly 4 in the prototype reported in [14], corresponding to 2 bits. Nevertheless, the best FoMs with this approach have been achieved in systems based on a multiple column (chain) encoder with four different

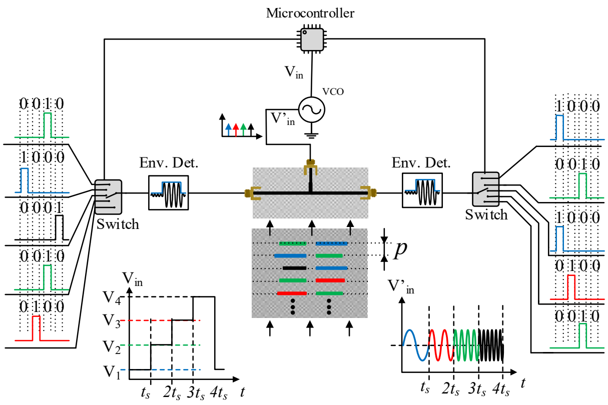

Figure 1. Sketch showing the working principle of the hybrid time/frequency domain encoder system based on a two-chain encoder and power splitter reader with two output ports. The VCO generates four harmonic signals, managed by a microcontroller, in order to detect the different sizes of the chain inclusions (frequency encoding is achieved through the size of the inclusions, as indicated in the text).

inclusions' sizes, and a reader implemented by means of a power splitter [15]. The sketch with a 1:2 power splitter reader and a two-column encoder is depicted in Fig. 1. Four harmonic signals tuned to the resonance frequencies of the inclusions (linear strips) must be alternately injected to the input port of the splitter by means of a VCO managed by a microcontroller. The ID information is contained in the envelope functions of such signals, retrieved from both output ports by means of envelope detectors and switches, as illustrated in Fig. 1. When a certain inclusion of any of the columns (or chains) is on top of corresponding line of the splitter, the signal at the frequency of that inclusion is not transmitted to the corresponding output port. Thus, we can detect and identify such inclusions from the dips in the envelope function for each harmonic feeding signal generated at the output ports. With this approach, the total number of states is 24 (= 5×5 − 1), corresponding to FoM = 4.58 bits per position. Note that for each column, there are 4 different states, or inclusions' sizes, plus the absence of inclusion, however the simultaneous absence of inclusion in both chains for a given position should be avoided, since at least one strip is required for the (necessary) synchronism of the encoder. This explains the above FoM.

Nevertheless, the best FoM was achieved in one of the prototypes reported in [15], with four encoder chains and a reader based on a 1:4 power splitter. The reader and a specific encoder are depicted in Fig. 2. With this system, the total number of different states per encoder position (or row) is 440, as justified in [15], corresponding to FoM = 8.78 bits per row, a competitive number. In brief, the states that can be discerned with each pair of chains at both sides of the splitter axis are depicted in Fig. 3. This corresponds to 21 states, which means that with the 4 column this number is 21×21 = 441. However, we should avoid the situation where all the strips of the four chains are absent, hence obtaining the above cited number of states and FoM.

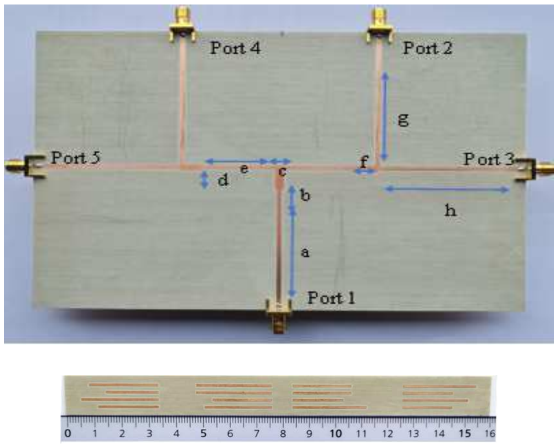

Figure 2. Photograph of the 1:4 power splitter reader and 4-row encoder. Dimensions of the reader (in mm) are: a = 51.5, b = 8.5, c = 4, d = 3, e = 27.5, f = 7, g = 58, h = 56. The period of the encoder is p = 0.3 cm. Dimensions of the access lines and distance between the different T-junctions, has been determined to accommodate displacement of the chains over the reader, namely, with two chains at both sides of access line of port 4 and two chains at both sides of access line of port 2. The reader and the encoder were implemented on the *Rogers 4003C* substrate with dielectric constant ε_r = 3.55, thickness h = 0.81 mm and loss factor tanδ = 0.0022. Reprinted from [15].

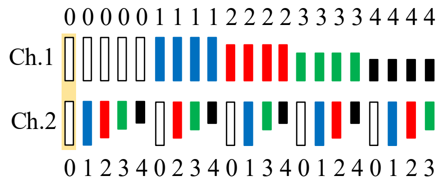

Figure 3. Possible combinations (21) of strips for the two pairs of chains of the encoder. Absence of strip is labeled as '0' and the other four labels correspond to the different strip lengths. Reprinted from [15].

Figure 4 shows the results for the encoder system of Fig 2 (the airgap was set to 0.5 mm). With the considered period (3 mm), the density of bits per unit length is DPL = 29.26 bit/cm, an unprecedentedly high value in this type of electromagnetic encoders.

2.2 Time/Phase Domain Encoders

In this approach, the encoder consists of a chain of inclusions (resonators, typically) located at different transverse positions. The reader is a one-port matched transmission line terminated with a matched load. When a resonator is on top of the reader line, the feeding signal, tuned to the resonators' resonance frequency, is reflected back in the resonator position, and the phase of the reflection coefficient depends on the distance between the input port and the line plane where the resonator is located. Thus, encoding is achieved through the phase of the reflection coefficient, modulated by the transverse position of the inclusions in the chain.

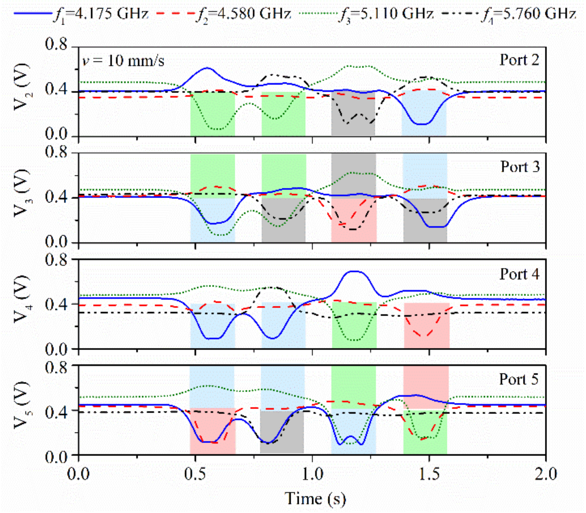

Figure 4. Envelope functions recorded at ports 2, 3, 4 and 5 for the encoder of Fig. 2. The frequencies of the inclusions, which are also the frequencies of the feeding signals, are indicated. Reprinted from [15].

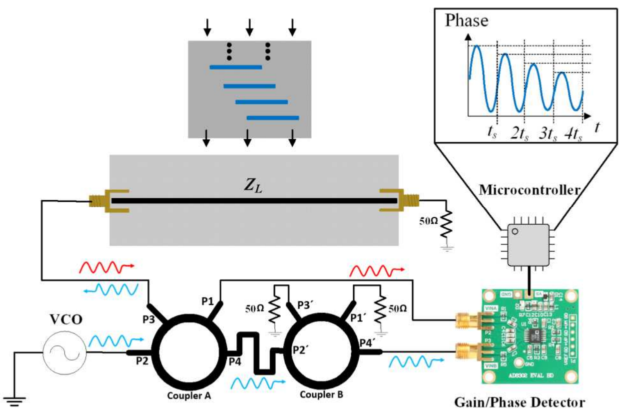

Figure 5. Sketch of the hybrid time/phase domain electromagnetic encoder system. The motion of the encoder over the reader line, at short vertical distance, is indicated by means of black arrows.

In [16], a time/phase domain encoder system was reported. The sketch is illustrated in Fig. 5, where it is shown that the phase of the reflection coefficient is retrieved by means of a pair of couplers and a gain/phase detector, as discussed in [16]. Figure 6 depicts the photograph of the reader line and three fabricated encoders, with 17 inclusions (linear strip resonators). The reader and encoders were fabricated on the *Rogers 4003C* substrate, with dielectric constant ε_r = 3.55, thickness h = 0.81 mm, and loss tangent tanδ = 0.0022. The dependence of the phase and magnitude of the reflection coefficient with time, as the encoder 1 is displaced over the reader is depicted in Fig. 7 (the airgap was set to 0.5 mm). The frequency of the feeding signal was set to 2.15 GHz. Synchronization is given by the maxima in the magnitude of the reflection coefficient, as discussed in detail in [16]. Figure 8 shows the phase for the three encoders but rearranged for an easy comparison. These results demonstrate that the measured phases do not depend on the specific sequence of strips in the chain.

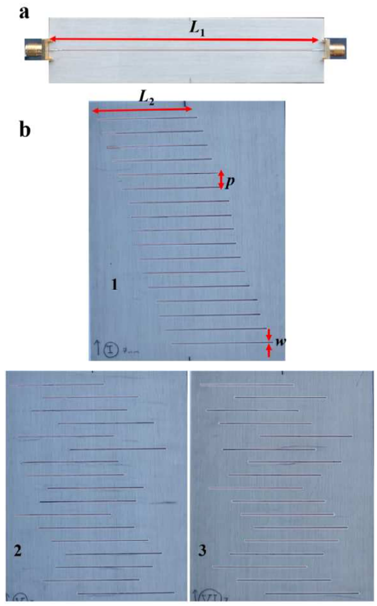

Figure 6. Photograph of the reader (a) and three hybrid time/phase domain encoders (b), with dimensions indicated. L_1 = 120 mm, L_2 =45 mm, p = 7mm, w = 0.5 mm.

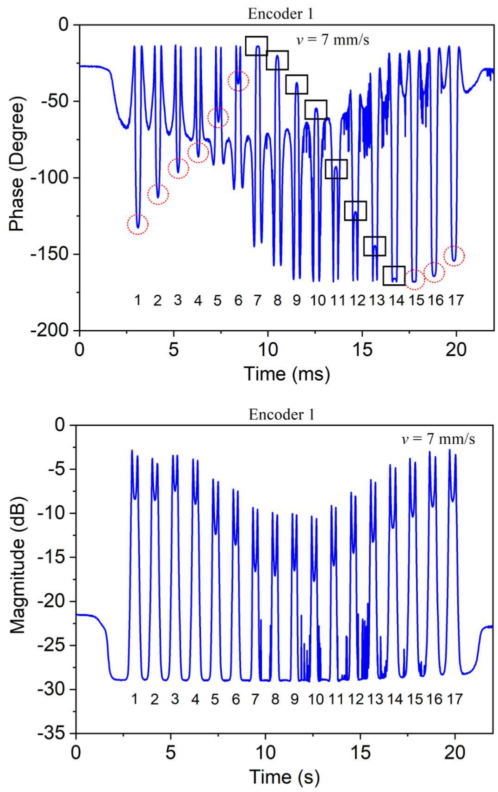

Figure 7. Measured phase and magnitude with time of the fabricated encoder 1 as it is displaced over the reader, as given by the gain/phase detector. Reprinted from [16].

With the encoder system of Fig. 6, the figure of merit is FoM = 4 bits per row. Since the period is 7 mm, the density of bits per unit length is DPL = 5.71 bit/cm. This result is not as good as the one corresponding to the hybrid time/frequency domain electromagnetic encoder system of Fig. 2, but the main advantage is that a single feeding signal

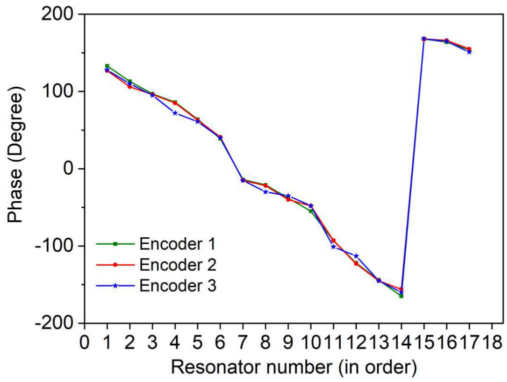

Figure 8. Measured phases for the encoders of Fig. 6, inferred dynamically with the gain/phase detector, by rearranging the phase values for easy comparison. Reprinted from [16].

suffices for encoder reading. Let us mention, to end this subsection, that we have recently implemented a system that exploits the time, the phase, and the frequency, where 6 bits per row have been achieved by means of a single reader line and a single frequency feeding signal [17]. However, this FoM can be doubled by considering two reader lines in parallel and two harmonic signals for retrieving the phase information.

3. Conclusions

It has been shown that the number of bits per row in electromagnetic encoders can be enhanced by encoding in the phase and/or in the frequency domains. The reported systems can be used as quasi-absolute encoders for motion sensing, or as near-field chipless-RFID tags.

6. Acknowledgements

This work was supported by MCIN/AEI 10.13039/501100011033, Spain (grants PID2022-139181OB-I00 and PRE2020-093239), and by ICREA.

References

[1] E. Eitel, "Basics of Rotary Encoders: Overview and New Technologies," *Machine Design Mag.*, vol. 4, no. 2, May. 2014.

[2] Z. Zhang, Y. Dong, F. Ni, M. Jin, and H. Liu, "A Method for Measurement of Absolute Angular Position and Application in a Novel Electromagnetic Encoder System," *J. Sensors*, Art. 503852, Apr. 2015.

[3] Z. Zhang, F. Ni, Y. Dong, M. Jin, and H. Liu, "A novel absolute angular position sensor based on electromagnetism," *Sens & Act., A: Phys.*, vol. 194, pp. 196-203, May. 2013.

[4] J. Jezný, and M. Curilla, "Position Measurement with Hall Effect Sensors", *Am. J. Mech. Eng.*, vol. 1, pp. 231–235, Jan. 2013.

[5] P.N. Granell, *et al.*, "Highly compliant planar Hall effect sensor with sub 200 nT sensitivity," *Npj Flex. Electron.*, vol. 3, p. 3, Feb. 2019.

[6] G. Scelba, *et al.*, "Fault-Tolerant Rotor Position and Velocity Estimation Using Binary Hall-Effect Sensors for Low-Cost Vector Control Drives," *IEEE Trans. Ind. Appl.*, vol. 50, pp. 3403–3413, Feb. 2014.

[7] G. Liu, B. Chen, and X. Song, "High-Precision Speed and Position Estimation Based on Hall Vector Frequency Tracking for PMSM with Bipolar Hall-Effect Sensors," *IEEE Sensors. J.*, vol. 19, pp. 2347–2355, Dec. 2018.

[8] C. Herrojo, *et al.*, "Near-Field Chipless-RFID System with High Data Capacity for Security and Authentication Applications," *IEEE Trans. Microw. Theory Techn.*, vol. 65, pp. 5298-5308, Dec. 2017.

[9] C. Herrojo, *et al.*, "Near-Field Chipless-RFID System with Erasable/Programmable 40-bit Tags Inkjet Printed on Paper Substrates," *IEEE Microw. Wireless Compon. Lett.*, vol. 28, pp. 272-274, Mar. 2018.

[10] C. Herrojo, F. Paredes and F. Martín, "Double-Stub Loaded Microstrip Line Reader for Very High Data Density Microwave Encoders," *IEEE Trans. Microw. Theory Techn.*, vol. 67, pp. 3527-3536, Sep. 2019.

[11] F. Martín, C. Herrojo, J. Mata-Contreras, F. Paredes, *Time-Domain Signature Barcodes for Chipless-RFID and Sensing Applications*, Springer, Feb. 2020.

[12] J. Mata-Contreras, C. Herrojo and F. Martín, "Detecting the Rotation Direction in Contactless Angular Velocity Sensors Implemented with Rotors Loaded with Multiple Chains of Resonators," *IEEE Sensors J.*, vol. 18, no. 17, pp. 7055-7065, Sep. 2018.

[13] F. Paredes, C. Herrojo and F. Martín, "Microwave Encoders with Synchronous Reading and Direction Detection for Motion Control Applications," *2020 IEEE/MTT-S Int. Microw. Symp.* (IMS), Los Angeles, CA, USA, 2020, pp. 472-475.

[14] A. Karami-Horestani, F. Paredes and F. Martín, "Frequency-Coded and Programmable Synchronous Electromagnetic Encoders Based on Linear Strips," *IEEE Sens. Lett.*, vol. 6, Art no. 3501704, Aug. 2022.

[15] A. Karami-Horestani, F. Paredes and F. Martín, "High Data Density Absolute Electromagnetic Encoders Based on Hybrid Time/Frequency Domain Encoding," *IEEE Sensors J.*, vol. 22, no. 24, pp. 23866-23876, Dec. 2022.

[16] A. Karami-Horestani, *et al.*, "Hybrid Time/Phase Domain Synchronous Electromagnetic Encoders for Near-Field Chipless-RFID and Motion Control Applications," *IEEE Trans. Microw. Theory Techn.*, vol. 71, pp. 5457-5469, Dec. 2023.

[17] A. Karami-Horestani, F. Paredes, and F. Martín, "Hybrid time/phase/frequency domain linear electromagnetic encoders for displacement sensing and near-field chipless RFID", *IEEE Journal RFID*, under review.